Journal of Orthopaedic Science xxx (xxxx) xxx

Contents lists available at ScienceDirect

Journal of Orthopaedic Science

journal homepage: http://www.elsevier.com/locate/jos

Original Article

Stress and strain changes of the anterior cruciate ligament at different knee flexion angles: A three-dimensional finite element study☆

Shaozheng Yang [1], Yongqiang Liu [1], Sushuang Ma [1], Chao Ding, Zhen Kong, Heng Li, Feng Huang, Hongfen Chen, Hua Zhong*

Department of Orthopaedics, The Fifth Affiliated Hospital, Southern Medical University, Guangzhou, Guangdong Province, 510999, China

ARTICLE INFO

Article history:
Received 30 July 2022
Received in revised form
23 April 2023
Accepted 12 May 2023
Available online xxx

Keywords:
Anterior cruciate ligament
Knee biomechanics
Knee flexion angles
Three dimensions finite element study

ABSTRACT

Objective: This study aimed to analyze the stress and strain changes of the anterior cruciate ligament (ACL) at different knee flexion angles using a three-dimensional finite element model.

Methods: Computed tomography and magnetic resonance imaging scans were performed on the right knee of 30 healthy adult volunteers. The imaging data were used to construct a three-dimensional finite element model of the knee joint. The magnitude and concentration area of stress and strain of ACL at knee flexion angles 0°, 30°, 60° and 90° were assessed.

Results: The magnitude of stress remained consistent at 0–30° ($P > 0.999$) and decreased at 30–90° ($P < 0.001$, $P = 0.005$, respectively), while the magnitude of strain increased between 0° and 30° ($P = 0.004$) and decreased between 30° and 90° ($P < 0.001$, $P = 0.004$, respectively). The stress concentration area remained consistent at the proximal end, midsubstance, and distal end between 0° and 60° ($P > 0.05$). The concentration area of strain increased at the proximal end, decreased at the midsubstance between 0° and 30°, and remained consistent between 30° and 90° ($P < 0.001$).

Conclusion: At the low knee flexion angle, ACL's magnitude of stress and strain reached the peak, and the concentration area of ACL strain gradually shifted from midsubstance to the proximal end.

1. Introduction

An anterior cruciate ligament (Anterior cruciate ligament, ACL) injury is a common sports injury of the knee [1]. In ACL injury, the knee is usually in low flexion angle, less in full extension and deep flexion angle [2,3]. Understanding the physiological function of the ACL during passive knee flexion may be an important step for future research on the mechanism of ACL injury. Therefore, some researchers applied the finite element method to study knee biomechanics and proved its feasibility [4–7]. The results in previous studies have also been controversial [4–6]. Some studies have reported that the role of the flexion angle in the ACL-induced stresses and strains was insignificant [5]; other studies suggesting that flexion angle has a significant effect on ACL stress have also reported different results [4,6]. But in previous studies, knee models were created by imaging the knee at different knee flexion angles, and almost all of them failed to include important auxiliary structures such as articular cartilage and meniscus [4,5]. In our study, imaging scans were performed only when the knee was fully extended, and then dynamic flexion was performed in a three-dimensional finite element model of the ground knee. At the same time, we considered meniscus and articular cartilage in constructing the knee joint model. This may allow a more realistic, objective and dynamic analysis of ACL biomechanics. In addition to ACL stress under different knee flexion angles, this study also compared ACL strain changes, which were not assessed in previous studies [4–6].

☆ Every person listed as an author has materially participated in the design, execution, and analysis of the study and verifies the accuracy of the entire manuscript before its submission.

* Corresponding author.
E-mail addresses: yangsz0713@163.com (S. Yang), 673813881@qq.com (Y. Liu), masushaung4437@163.com (S. Ma), nfwydingchao@163.com (C. Ding), 624868650@qq.com (Z. Kong), 982406737@qq.com (H. Li), 181014009@qq.com (F. Huang), aricalchf@126.com (H. Chen), zhong8099@163.com (H. Zhong).

[1] The first three authors contributed equally to this manuscript.

https://doi.org/10.1016/j.jos.2023.05.015

Please cite this article as: S. Yang, Y. Liu, S. Ma *et al.*, Stress and strain changes of the anterior cruciate ligament at different knee flexion angles: A three-dimensional finite element study, Journal of Orthopaedic Science, https://doi.org/10.1016/j.jos.2023.05.015

This study aimed to analyze the stress and strain changes of the ACL at different knee flexion angles using a three-dimensional finite element model. The hypothesis was that ACL's magnitude and concentration area of stress and strain change significantly with knee flexion between 0° and 90°.

2. Methods

Thirty healthy adult volunteers were recruited for the study between July 2021 and January 2022. The study was approved by our institutional review board, and participants signed informed consent forms. Inclusion criteria included age 18—55 years and radiographic evidence of epiphyseal closure. Exclusion criteria included a history of knee disease (osteoarthritis, meniscus injury, ligament injury, inflammatory disease, etc.), knee surgery, and systemic metabolic diseases. 64-slice computed tomography (CT) and 3.0T magnetic resonance imaging (MRI) scans were performed on the volunteers' right knee while they were in the supine position (the patient had a straight leg axis). CT scanner (Aquilion, Toshiba, Japan): 150 KV; 120 mA; slice thickness, 1 mm; scanning range from the upper margin of the patella to the fibula head. MRI scanner (Discovery750w, GE, America): repetition time, 13.6 ms; echo time, 2/Fr; numbers of excitation, 4; matrix, 416*320; field of view, 18 × 18 cm. The imaging data were used to construct a three-dimensional finite element model of the knee joint, including the ACL employing several modeling programs. Then the knee joint was dynamically flexed in this three-dimensional finite element model, and the changes of stress and strain were recorded at different knee flexion angles. The data of 20 points with maximum stress and strain of ACL at knee flexion angles of 0°, 30°, 60° and 90° were extracted for statistical analysis. In addition, the concentrated areas of stress and strain changes were reported as proximal end, midsubstance, and distal end [8,9]. 10% of the entire ACL length close to the femoral and tibial insertion was considered the proximal and distal ends, respectively, and the midsubstance was the interval between the proximal and distal ends [10].

2.1. Main equipment and related software

Major imaging equipment: MRI scanner (Discovery750w, GE, America), CT scanner (Aquilion, Toshiba, Japan), Digital radiography (Definium 6000, GE, America).

Computer configuration: DELL Precision T7920 tower graphics workstation (CPU Intel Xeon Gold 61262.6G12 core processor, 64G memory, 256G SSD+6 TB SATA disk).

Main experimental software: Mimics 15.0 (Materialize, Belgium), Geomagic Studio 2013 (Raindrop, America), Solidworks2018 (Dassault, France), Abaqus 2018 (Dassault, France).

2.2. Part model of knee joint

The knee CT and MRI image files were imported into Mimics 15.0 (Materialize, Belgium) software. The region growth and hand-edit layer tools were used to disconnect non-existent connections between areas, erase excess parts, or fill in missing parts. Finally, initial part models of the femur, tibia, meniscus, cartilage and ligament were generated (Fig. 1). After smoothing the model, it was exported and saved in stereolithography format and then imported

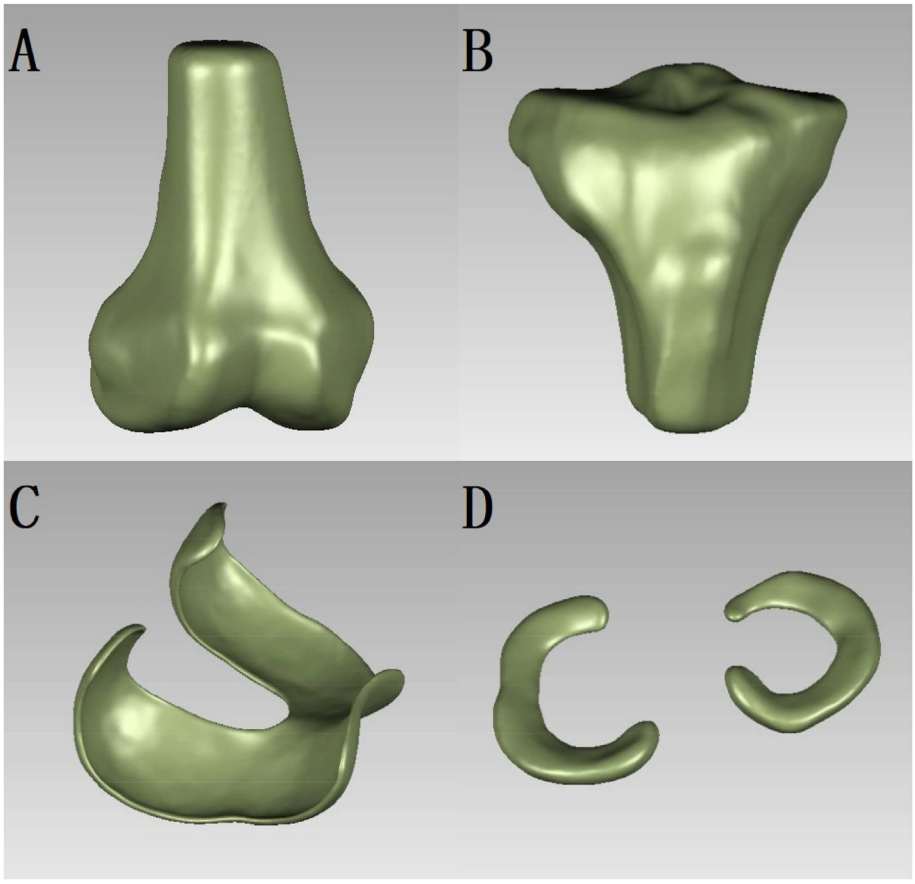

Fig. 1. Reconstructed part model of the right knee joint. (A) Show the anterior view of the model of the right femur. (B) Show the anterior view of the model of the right tibia. (C) Show the overhead view of the cartilage model of the right femur. (D) Show the overhead view of the meniscus model of the right knee.

into Geomagic Studio 2013 (Raindrop, America) software for conversion into a polygonal model consisting of many triangular meshes. The triangular mesh of the uneven position on the model surface was manually deleted, and holes in the deleted position were filled. After the model was optimized and smoothed, contour lines were generated on the model by the automatic contour detection function of the precise surface module. Deformed or unreasonable contours were edited and modified. Then, the surface slices were constructed with reference to the contour lines and the intersecting boundary line on the surface slices was modified. The qualified surface slices were used to build the grid and automatically repair the grid in the intersection area. The grid was fitted to produce a 3 dimensions surface with smooth curvature. Eventually, the fitted surface was derived as geometric models in the X_T general format.

2.3. Three-dimensional solid model

The geometry models saved in X_T general format were imported into the Solidworks 2018 (Dassault, France) software separately, and the problematic surfaces were repaired according to the software's hints. Each model was saved in Solidworks format and imported into the Solidworks assembly. According to the locations of each part of the knee obtained from CT and MRI imaging data, the bone, cartilage, meniscus and ligament models were assembled through the origin match command to form a preliminary complete knee model. The position of the femur and tibia is limited by ligaments, meniscus, and cartilage. The entire model was saved as a Solidworks parts file format and opened in the Solidworks parts module. The overlapping parts of the articular cartilage and bone were removed by the combination command through the Boolean difference method so that the surface contour of the articular cartilage was closely fitted with the bone surface. The ligaments were treated with the same method. The three-dimensional solid knee joint model conforming to finite element analysis was established and saved in X_T format (Fig. 2).

2.4. Three-dimensional finite element model

The three-dimensional solid knee joint model was imported into Abaqus 2018 (Dassault, France) finite element analysis software. The material parameters of the femur, tibia, meniscus, cartilage and ligament were established in the analysis properties and were assigned to each model [11,12] (Table 1). The analysis type was defined as dynamic explicit analysis in the analysis step. Then the contact relationship between the models was defined. The contact type between cartilage and meniscus was set to frictionless contact. All other contact types were fixed. Boundary conditions and loads were then set (Fig. 3). During loading, force is transferred between the femur and tibia through ligaments, meniscus, and cartilage. The lower surface of the tibia was set to a fully fixed constraint when gravity loads were applied, and a weight gravity load was applied to the femur end face in a vertical downward direction. The bending load is applied to the upper end of the femur in a backward direction. However, when the bending load is applied, dynamic bending from 0° to 90° can be performed directly by setting the rotation angle, without the need to apply a torque with a specific value. The next step was to mesh the model. The mesh type was tetrahedral mesh C3D4. The global size of the grid was defined as 2.5 mm, and the local edge size was 1.2 mm. The number of nodes and cells was 67,870 and 314,211, respectively (Fig. 4). Finally, the analysis job was created, and the calculation was submitted.

Table 1
Material properties of each part of the model.

Structure	Modulus of elasticity (MPa)	Poisson's ratio
Femur	3883.4	0.3
Tibia	4184.6	0.3
Meniscus	59	0.49
Cartilage	20	0.46
Anterior cruciate ligament	116	0.3
Posterior cruciate ligament	87	0.3
Medial collateral ligament	48	0.3
Lateral collateral ligament	48	0.3

Note: References: [11]. Otani, T., Y. Kobayashi and M. Tanaka, Computational study of kinematics of the anterior cruciate ligament double-bundle structure during passive knee flexion-extension. Med Eng Phys, 2020-09-01. 83: p. 56–63 [12]. Marouane, H., A. Shirazi-Adl and J. Hashemi, Quantification of the role of tibial posterior slope in knee joint mechanics and ACL force in simulated gait. J Biomech, 2015-07-16. 48(10): p. 1899–905.

2.5. Statistical analyses

SPSS 22.0 (version 22.0; SPSS, Chicago, IL, USA) software for Windows was used for statistical analysis. Fisher's exact probability

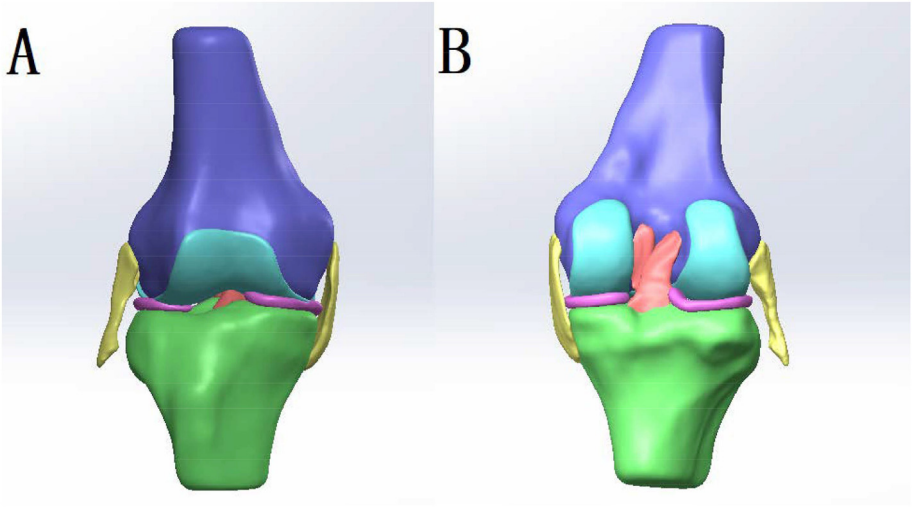

Fig. 2. Reconstructed three-dimensional solid model of the right knee joint. (A) Show the anterior view of the three-dimensional solid model of the right knee joint. (B) Show the posterior view of the three-dimensional solid model of the right knee joint.

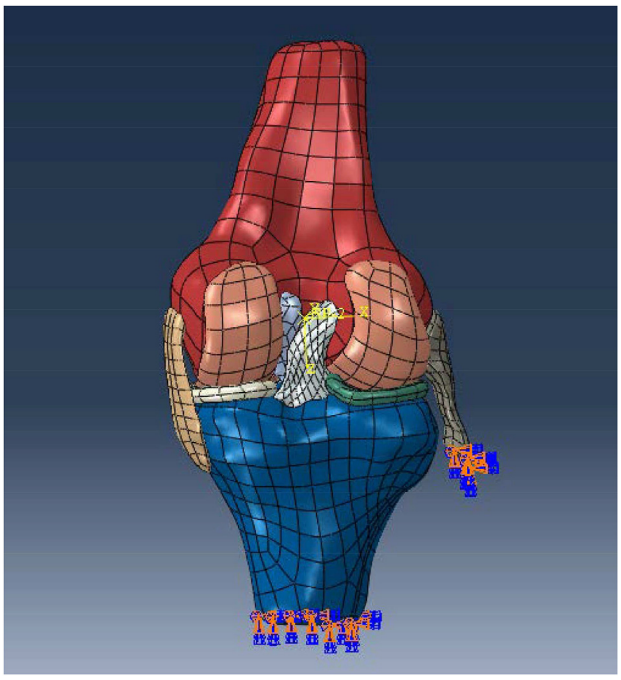

Fig. 3. The boundary conditions and loads of the right knee joint model are set.

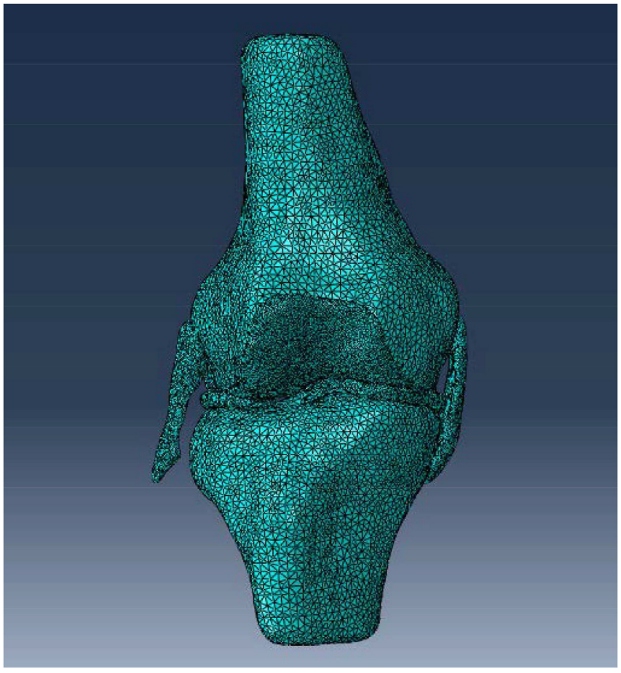

Fig. 4. The right knee joint model meshed.

method was used to compare the concentration area of stress and strain at different knee flexion angles. Shapiro-Wilk test was used to determine whether the magnitude of stress and strain at different knee flexion angles followed the normal distribution. The magnitude of height, weight, stress and strain at all knee flexion angles (except the magnitude of stress at 0° knee flexion) conformed to a normal distribution and were expressed as mean ± standard deviation. The magnitude of age, body mass index (BMI) and stress at 0° knee flexion did not conform to a normal distribution and were expressed as mean (25%, 75%). The magnitude of stress and strain at different knee flexion angles did not conform to normal distribution or homogeneity of variance and were compared using the Kruskal-Wallis Test. The level of statistical significance was set at $P < 0.05$.

3. Results

The 30 healthy adult volunteers included 19 males and 11 females, aged 33 (25, 42) years, height 171.70 ± 7.18 cm, weight 63.13 ± 7.73 kg, and BMI 22.55 (21.40, 23.31) kg/cm^2.

During knee flexion, the magnitude of ACL stress remained consistent between 0° and 30° ($P > 0.999$) and decreased between 30° and 90° ($P < 0.001$, $P = 0.005$, respectively), while the magnitude of ACL strain increased between 0° and 30° ($P = 0.004$) and decreased between 30° and 90° ($P < 0.001$, $P = 0.004$, respectively) (Table 2).

During knee flexion, the concentration area of ACL stress remained consistent at the proximal end, midsubstance, and distal end between 0° and 60° ($P < 0.001$), increased at the proximal end, decreased at the midsubstance and remained consistent at the distal end from 60° to 90° ($P < 0.001$) (Table 3, Figs. 5 and 6). During knee flexion, the concentration area of ACL strain increased at the proximal end, decreased at the midsubstance between 0° and 30°, and both remained consistent between 30° and 90° ($P < 0.001$); while the concentration area of ACL strain always remained consistent at the distal end between 0° and 90° ($P > 0.05$) (Table 4, Figs. 5 and 7).

4. Discussion

Some studies have reported low flexion angle as the typical knee posture for ACL injury [2,3]. Besides, ACL ruptures were observed arthroscopically, most frequently at the femoral insertion site (proximal tear) [5,8,13]. The motion of the knee joint is complex, and the biomechanical mechanism of ACL is also varied. Biomechanical research through the traditional cadaveric model is undoubtedly the most intuitive [14]. However, the tissue structure of the isolated joint model will degenerate, which may be affected by the preservation time and method of the cadaver, which may affect the test results. With the continuous development of biomechanics, material science and computer technology, the application of the finite element method in the study of knee biomechanics is becoming more mature. In recent years, several finite element model studies have analyzed the ACL stress changes under different knee flexion angles, but there are contradictions in their conclusions [4–6]. We made some improvements in the study design.

Table 2
The stress and strain of the anterior cruciate ligament (ACL) at different knee flexion angles.

	0°	30°	60°	90°	P
Stress (MPa)	52.53 (48.54, 57.95)	55.54 ± 2.35	24.99 ± 2.16^{ab}	14.71 ± 1.75^{abc}	<0.001
strain (%)	15.14 ± 2.01	23.53 ± 1.83^{a}	9.61 ± 1.93^{ab}	3.61 ± 0.77^{abc}	<0.001

Note: Statistically significant difference ($P < 0.05$) compared with ^{a}0°, ^{b}30°, and ^{c}60°.

Table 3
The concentrated areas of stress changes of the anterior cruciate ligament (ACL) at different knee flexion angles.

	0°	30°	60°	90°	Total
Proximal (n)	0[a]	0[a]	2[a]	13[b]	15
Midsubstance (n)	28[a]	30[a]	28[a]	17[b]	103
Distal (n)	2[a]	0[a]	0[a]	0[a]	2
Total	30	30	30	30	120

Note: The Fisher's exact probability method was used to compare the concentration area of stress at different knee flexion angles. $Z = 32.03$, $P < 0.001$.
Each superscript letter indicates a subset of Group categories whose column proportions are not significantly different from each other at level 0.05.

First, instead of taking imaging scans under different knee flexion angles, imaging scans were performed only when the knee was fully extended, and then dynamic flexion was performed in a 3D finite element model of the ground knee, which could objectively and dynamically simulate the biomechanical changes of ACL more. Secondly, we did not neglect the meniscus and articular cartilage as in previous studies. Considering articular cartilage and meniscus in the finite element model can reflect the biomechanical mechanism of ACL more truly. The meniscus is a very important stabilizing structure of the knee joint, and the thickness between the femur and tibia has been shown to be closely related to ACL stress [15,16]. Finally, in addition to ACL stress at different knee flexion angles, changes in ACL strain that better reflect ACL tears were also included in this study. The results confirmed our hypothesis. The most important finding of this study was that at the low knee flexion angle, the ACL magnitude of stress and strain reached the peak, and its strain concentration area gradually shifted from midsubstance to the proximal end.

Based on the three-dimensional finite element model, the biomechanical research of ACL has attracted extensive attention in recent years [4–7]. It has been proposed in previous three-dimensional finite element studies that the ACL has the maximum stress at low knee flexion angles [4,5]. This proposition is consistent with our findings. Studies have shown that the Lachman test (30° knee flexion angle) is more accurate and sensitive than the anterior drawer test (90° knee flexion angle) in the diagnosis of ACL injury, especially in acute injury [17,18]. It may also be that ACL stress is greater at 30° than at 90°. Some studies have suggested that the flexion angle is insignificant in inducing stresses and strains of the ACL, implying the same chance of ACL injury in various daily activities, i.e., walking, climbing stairs, sitting, etc. [5,19]. However, this conflicts with our results and is inconsistent with our clinical observations. In our study, the magnitude of ACL stress remained consistent between 0° and 30° and decreased between 30° and 90°. Some studies have reported similar results. Kim evaluated the stress and strain changes of the reconstructed ACL using the finite element model and proposed that the strain and stress of the ACL reached the maximum at full extension and decreased at 45–90° [4]. We analyzed the possible causes of this contradiction. In the previous study, the sample size was only 1 case, which could not rule out the interference of chance, and only the results of knee flexion between 0° and 45° were analyzed [5]. In our study, the difference in ACL stress was not significant at 0–30° knee flexion but significant between 30° and 60° knee flexion. When the

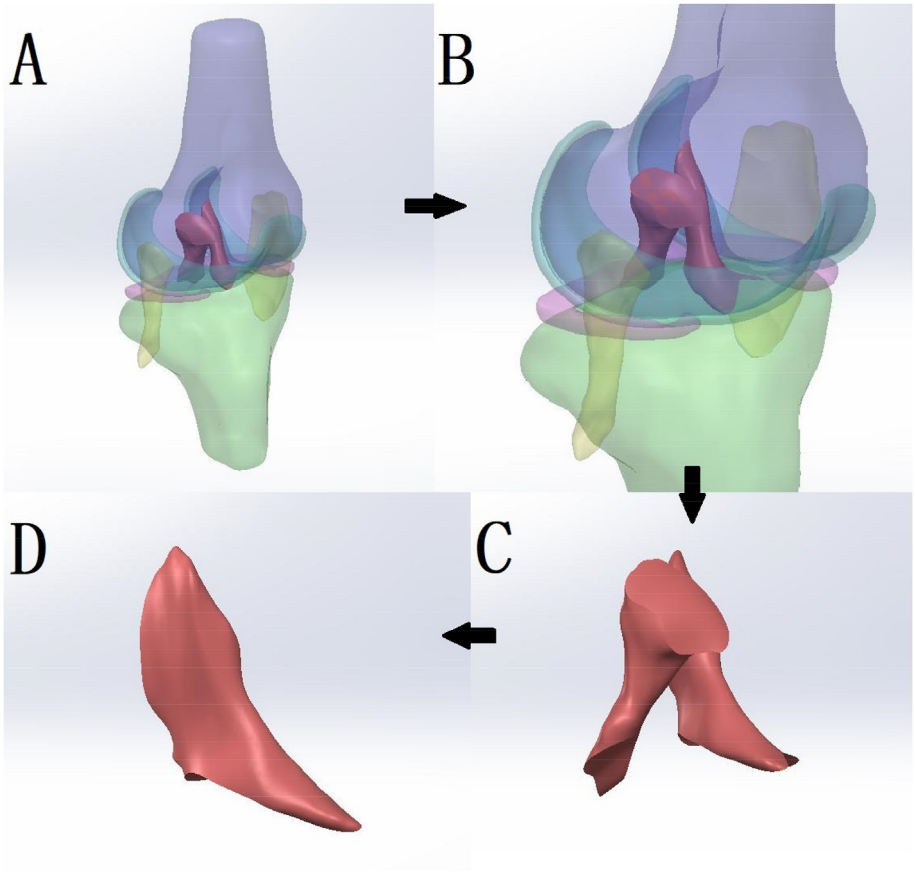

Fig. 5. The bone attachment surface and the orientation of anterior cruciate ligaments (view from antero-medial knee aspect). (A) The oblique view of knee joint model. (B) Enlarge the oblique view of knee joint model. (C) The anterior and posterior cruciate ligaments are extracted. (D) The anterior cruciate ligaments are extracted.

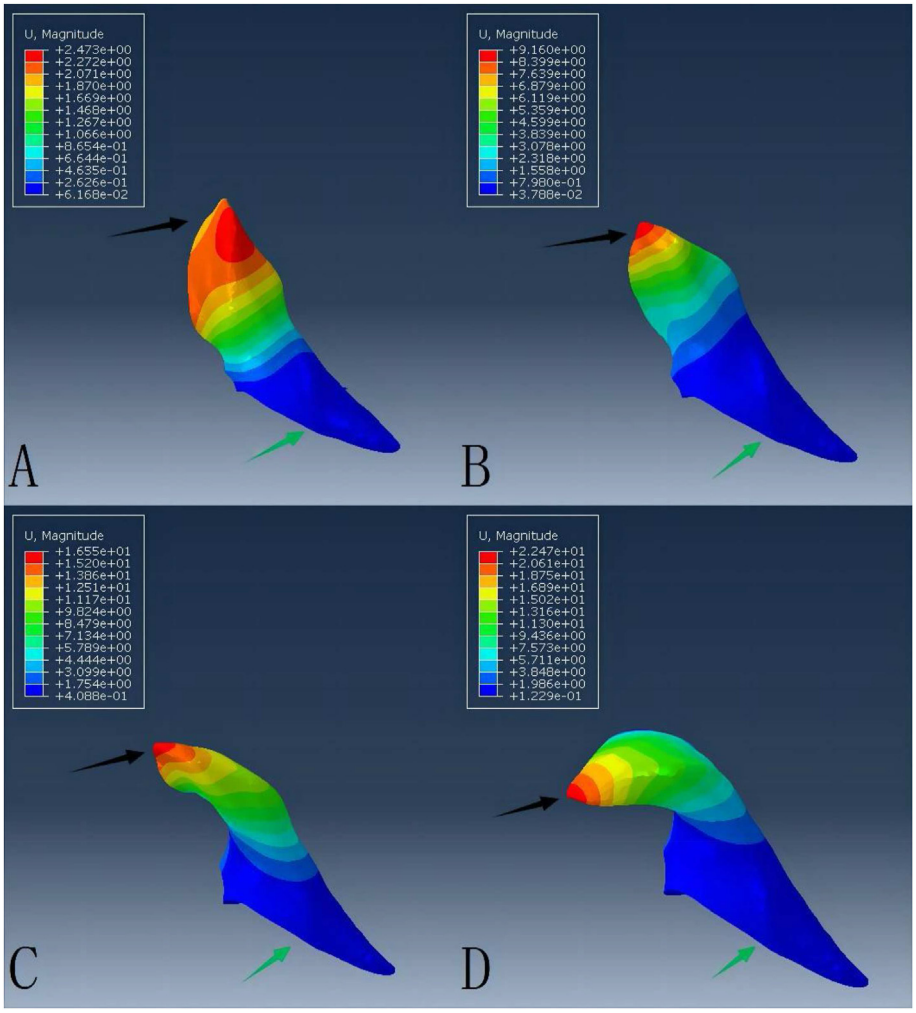

Fig. 6. Output the corresponding stress nephogram to determine the ACL stress distribution concentration area. The black arrow indicates the proximal attachment of the ACL (femoral foot print). The green arrow indicates the distal attachment of the ACL (tibial foot print). (A) The stress nephogram at 0° knee flexion. (B) The stress nephogram at 30° knee flexion. (C) The stress nephogram at 60° knee flexion. (D) The stress nephogram at 90° knee flexion. (For interpretation of the references to color in this figure legend, the reader is referred to the Web version of this article.)

grouping range of knee flexion angle is not large enough, there may be no significant difference in the results.

The most common site of ACL tear was reported to be the femoral insertion site (proximal tear) [5,8,13]. In our study, when knee flexion angles were 30°, 60° and 90°, the concentration area of ACL strain was at the proximal end. At 30° of knee flexion, both ACL stress and strain reached the peak value, and the concentration of ACL strain was located at the femoral insertion position. Therefore, we hypothesized that ACL injury might likely occur at a knee flexion of 30°. Multi-plane loading, namely the tibial forward loading associated with valgus, protonation and low flexion angle of the knee, is considered the mechanism of ACL injury [20]. We found an interesting phenomenon: at 30–60° of knee flexion, the concentration areas of stress and strain were located in the midsubstance and proximal of the ACL, respectively, but not in the same position. Theoretically, the greater the stress, the greater the strain. The changes of stress and strain are different in this study. The premise that the stress and strain are linearly proportional is that the material model is a straight line model with the same cross-sectional area. Every part of the material has the same elastic coefficient, so that the greater the stress, the greater the strain. However, the ACL is a fiber bundle model with narrow middle and wide sides, rather than a straight line model with the same cross-sectional area. So the stress and strain change differently. It is suggested that the stress concentration area during knee flexion is mainly in the proximal and midsubstance of ACL [5]. However, there are few studies on the concentrated areas of strain. Specific reasons are unclear, and few studies have explained them. It is proposed that the fiber orientations in ACL are almost parallel when the knee flexion angle is 0°, but it will become twisted and curved when the knee flexion angle increases [11]. This may cause the part with less fiber in the same direction to tear when subjected

Table 4
The concentrated areas of strain changes of the anterior cruciate ligament (ACL) at different knee flexion angles.

	0°	30°	60°	90°	Total
Proximal (n)	5^a	28^b	29^b	29^b	91
Midsubstance (n)	25^a	2^b	1^b	1^b	29
Total	30	30	30	30	120

Note: The Fisher's exact probability method was used to compare the concentration area of strain at different knee flexion angles. $Z = 69.05$, $P < 0.001$.
Each superscript letter indicates a subset of Group categories whose column proportions are not significantly different from each other at level 0.05.

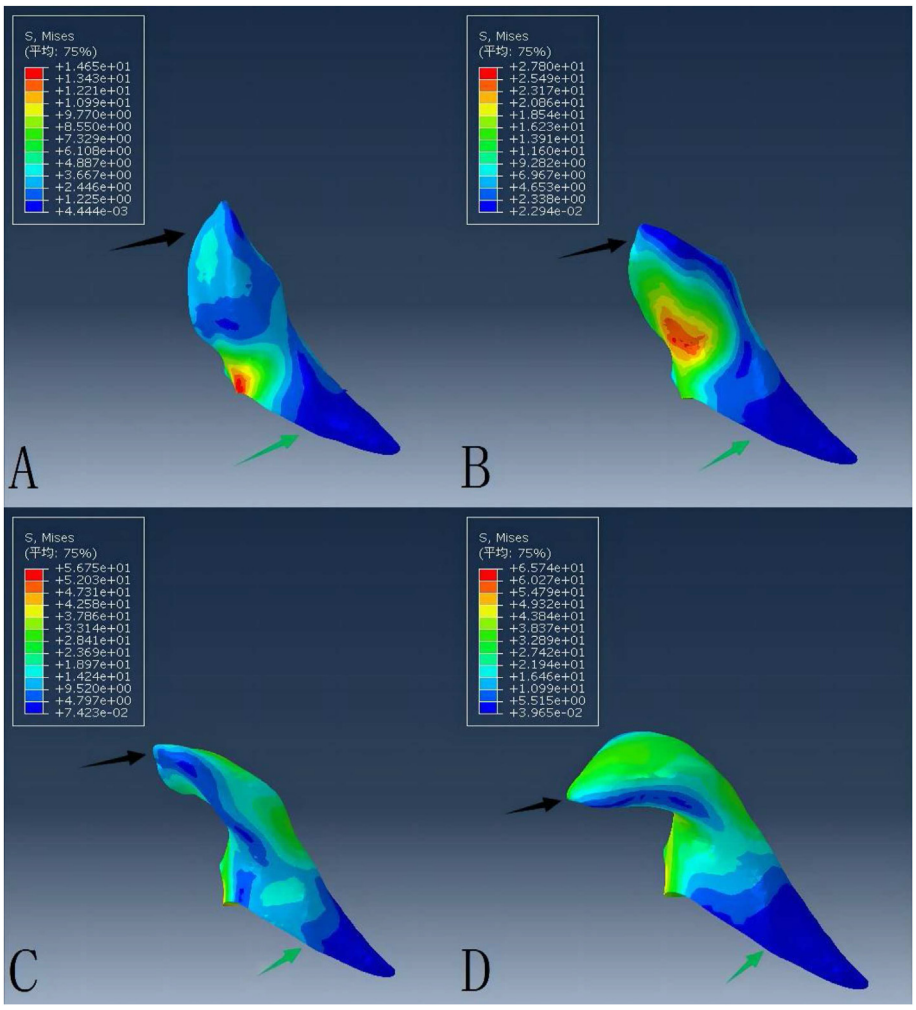

Fig. 7. Output the corresponding strain nephogram to determine the ACL strain distribution concentration area. The black arrow indicates the proximal attachment of the ACL (femoral foot print). The green arrow indicates the distal attachment of the ACL (tibial foot print). (A) The strain nephogram at 0° knee flexion. (B) The strain nephogram at 30° knee flexion. (C) The strain nephogram at 60° knee flexion. (D) The strain nephogram at 90° knee flexion. (For interpretation of the references to color in this figure legend, the reader is referred to the Web version of this article.)

to lower stress, while the part with more fiber in the same direction may not tear when subjected to higher stress.

Analyzing the stress and strain of ACL under different knee flexion angles helps elucidate the ACL injury mechanism and guide its reconstruction. During ACL reconstruction, the graft is typically fixed at 0°−30°. This ensures that maximum stress can be obtained during graft fixation to avoid further increase in graft stress during knee flexion and extension leading to graft tear or limited knee motion. It also plays an important role in preventing ACL injury, especially during landing and cutting, and encouraging greater angle knee flexion may reduce the risk of ACL injury [20].

4.1. Limitations

There are some limitations to this study. First, the knee load is dynamic change rather than static in the process of walking. In this model we simply applied the body weight gravity load. The current research has not been able to dynamically apply loads according to load changes during walking [5]. Secondly, ACL stresses and strains were analyzed and calculated only at 0°, 30°, 60°, and 90° knee flexion angles in our study, and the deeper flexion angles were not included. However, ACL injury rarely occurs at deep knee flexion angles [2,3]. Last, although bone, cartilage, meniscus and major ligaments were considered, the muscles, nerves and secondary ligaments around the knee were also neglected for technical reasons. These structures are also important factors affecting ACL stress and strain.

5. Conclusions

At the low knee flexion angle, ACL's magnitude of stress and strain reached the peak, and the concentration area of ACL strain gradually shifted from midsubstance to the proximal end.

Ethics approval and consent to participate

The present study was approved by The Fifth Affiliated Hospital, Southern Medical University.

Source of funding

The authors received no financial support from any institution, organization, or individual.

Conflicts of interest

The authors report no conflicts of interest.

Acknowledgments

The authors acknowledge the surgical staff at The Fifth Affiliated Hospital, Southern Medical University.

References

[1] Lucarno S, Zago M, Buckthorpe M, Grassi A, Tosarelli F, Smith R. et al. Systematic video analysis of anterior cruciate ligament injuries in professional female soccer players. Am J Sports Med 2021 Jun 1;49(7):1794–802.
[2] Owusu-Akyaw KA, Kim SY, Spritzer CE, Collins AT, Englander ZA, Utturkar GM, et al. Determination of the position of the knee at the time of an anterior cruciate ligament rupture for male versus female patients by an analysis of bone bruises. Am J Sports Med 2018 Jun 1;46(7):1559–65.
[3] Sasaki S, Koga H, Krosshaug T, Kaneko S, Fukubayashi T. Kinematic analysis of pressing situations in female collegiate football games: new insight into anterior cruciate ligament injury causation. Scand J Med Sci Sports 2018 Mar 1;28(3):1263–71.
[4] Kim HY, Seo YJ, Kim HJ, Nguyenn T, Shetty NS, Yoo YS. Tension changes within the bundles of anatomic double-bundle anterior cruciate ligament reconstruction at different knee flexion angles: a study using a 3-dimensional finite element model. Arthroscopy 2011 Oct 1;27(10):1400–8.
[5] Safari M, Shojaei S, Tehrani P, Karimi A. A patient-specific finite element analysis of the anterior cruciate ligament under different flexion angles. J Back Musculoskelet Rehabil 2020 Jan 20;33(5):811–5.
[6] Limbert G, Middleton J, Taylor M. Finite element analysis of the human ACL subjected to passive anterior tibial loads. Comput Methods Biomech Biomed Eng 2004 Feb 1;7(1):1–8.
[7] Vairis A, Stefanoudakis G, Petousis M, Vidakis N, Tsainis AM, Kandyla B. Evaluation of an intact, an ACL-deficient, and a reconstructed human knee joint finite element model. Comput Methods Biomech Biomed Eng 2016 Feb 1;19(3):263–70.
[8] Zantop T, Brucker PU, Vidal A, Zelle BA, Fu FH. Intraarticular rupture pattern of the ACL. Clin Orthop Relat Res 2007 Jan 1;454:48–53.
[9] DeHaven KE. Diagnosis of acute knee injuries with hemarthrosis. Am J Sports Med 1980 Jan 1;8(1):9–14.
[10] Girgis FG, Marshall JL, Monajem A. The cruciate ligaments of the knee joint. Anatomical, functional and experimental analysis. Clin Orthop Relat Res 1975 Jan 1;(106):216–31.
[11] Otani T, Kobayashi Y, Tanaka M. Computational study of kinematics of the anterior cruciate ligament double-bundle structure during passive knee flexion-extension. Med Eng Phys 2020 Sep 1;83:56–63.
[12] Marouane H, Shirazi-Adl A, Hashemi J. Quantification of the role of tibial posterior slope in knee joint mechanics and ACL force in simulated gait. J Biomech 2015 Jul 16;48(10):1899–905.
[13] Grassi A, Nitri M, Moulton SG, Marcheggiani MG, Bondi A, Romagnoli M, et al. Does the type of graft affect the outcome of revision anterior cruciate ligament reconstruction? a meta-analysis of 32 studies. Bone Joint Lett J 2017 Jun 1;99-B(6):714–23.
[14] Ahn JH, Koh IJ, McGarry MH, Patel NA, Lin CC, Lee TQ. Double-bundle anterior cruciate ligament reconstruction with lateral extra-articular tenodesis is effective in restoring knee stability in a chronic, complex anterior cruciate ligament-injured knee model: a cadaveric biomechanical study. Arthroscopy 2021 Jul 1;37(7):2220–34.
[15] Kia M, Warth LC, Lipman JD, Wright TM, Westrich GH, Cross MB, et al. Fixed-bearing medial unicompartmental knee arthroplasty restores neither the medial pivoting behavior nor the ligament forces of the intact knee in passive flexion. J Orthop Res 2018 Jul 1;36(7):1868–75.
[16] Forkel P, von Deimling C, Lacheta L, Imhoff FB, Foehr P, Willinger L, et al. Repair of the lateral posterior meniscal root improves stability in an ACL-deficient knee. Knee Surg Sports Traumatol Arthrosc 2018 Aug 1;26(8):2302–9.
[17] Sobrado MF, Bonadio MB, Ribeiro GF, Giglio PN, Helito CP, Demange MK. Lever sign test for chronic ACL injury: a comparison with lachman and anterior drawer tests. Acta Ortopédica Bras 2021 May 1;29(3):132–6.
[18] Zhao GL, Lyu JY, Liu CQ, Wu JG, Xia J, Huang GY. A modified anterior drawer test for anterior cruciate ligament ruptures. J Orthop Surg Res 2021 Apr 14;16(1):260.
[19] Mesfar W, Shirazi-Adl A. Biomechanics of the knee joint in flexion under various quadriceps forces. Knee 2005 Dec 1;12(6):424–34.
[20] Otsuki R, Benoit D, Hirose N, Fukubayashi T. Effects of an injury prevention program on anterior cruciate ligament injury risk factors in adolescent females at different stages of maturation. J Sports Sci Med 2021 Jun 1;20(2):365–72.